10.1007/s12541-009-0104-2

Modeling of Bending Behavior of IPMC Beams Using Concentrated Ion Boundary Layer

Waqas Akbar Lughmani[1], Jae Young Jho[2], Jang Yeol Lee[2] and Kyehan Rhee[1,#]

1 Department of Mechanical Engineering, Myongji University, 38-2, Nam-dong, Yongin, Kyunggi-do, South Korea, 419-723
2 Department of Chemical and Biological Engineering, Seoul National University, 599, Kwanag-ro, Kwanag-gu, Seoul, South Korea, 151-742
Corresponding Author / E-mail: khanrhee@mju.ac.kr, TEL: +82-31-330-6426, FAX: +82-31-321-4959

KEYWORDS: IPMC, Concentration boundary layer, FEM, Bending, Catheter

Ionic polymer metal composites (IPMCs) are an emerging class of electroactive polymers (EAP), which have many potential applications as sensors and actuators. Recently, IPMCs have been intensively studied because of their huge potential in medical, mechanical, electronic, and aerospace engineering. However, before the benefits of these materials can be effectively exploited for practical use, a mathematical model must be established to enhance understanding and predictability of IPMC actuation. The coupled electrical-chemical-mechanical response of an IPMC depends on the structure of the polyelectrolyte membrane, the morphology and conductivity of the metal electrodes, the cation properties, and the level of hydration. With this in mind, the purpose of this study is to establish a finite element model for bending behavior of IPMC beams. With reference to their operation principle, it is assumed that an IPMC beam has three virtual layers. We draw an analogy between thermal strain and real strain in IPMC due to volume change. This is a coupled structure/thermal model, and the finite element method is used to solve this model. The ion concentration distribution in the IPMC boundary layer is mimicked with the temperature distribution, and the electromechanical coupling coefficient is mimicked with the thermal expansion coefficient. Theoretical and experimental results demonstrate that our suggested model is practical and effective enough in predicting the blocking force of IPMC strips for different input voltages and strip thicknesses.

Manuscript received: August 28, 2008 / Accepted: May 7, 2009

1. Introduction

Ionic polymer metal composites (IPMCs) are innovative materials belonging to the class of ionic electroactive polymers.[1] A typical IPMC consists of a polyelectrolyte membrane (usually Nafion or Flemion) plated on both faces by a noble metal, and is neutralized with certain counter ions that balance the electrical charge of the anions covalently fixed to the back-bone membrane. Transport of hydrated cations within an IPMC beam under the applied voltage and associated electrostatic interactions lead to bending of an IPMC beam. Fig. 1 illustrates the cross-section of the Nafion based IPMC beam and its actuation mechanism. Since it produces large bending motion under low actuation voltage with good biocompatibility and resiliency, an IPMC beam has tremendous application in biomedical devices and biomimetic robotics.[2-9] Microfabrication of IPMC[10] has also been reported, which extends IPMC applications into the micro and nano manipulation domain.

Prediction of the electro-mechanical behavior of IPMCs is important in many biomedical and MEMS devices, but the analytical approach to solving the complex electro-mechanical behavior of a composite material is very limited. To solve the problem with computational methods, mathematical modeling of an IPMC has been attempted. Generally, IPMC models are categorized as white box models (physical models) and black box models (empirical models). Physical models are based on the physics and chemistry involved in IPMC deformation. For these models, researchers select and model the set of underlying mechanisms that the researchers believe to be responsible for the electromechanical response and subsequent deformation (actuation) or sensing (electrical output). Shahinpoor[11] and Nemat-Nasser *et al*[12,13] proposed physical models, and Johnson and Amirouche[14] have

developed a multiphysics model based on the electro-thermal behavior of the actuation of IPMC. These models predicted IPMC behavior quite accurately, but they require many physical and chemical properties that must be determined through experiments. For the black box models, also called empirical models, the physical features are only a minor consideration, and the model parameters are based on system identification. Wang *et al*[15] and Xiao *et al*[16] estimated forces and deformations of IPMCs through this approach, but these approaches are applicable only to specific shapes and operation conditions due to their empirical nature. Based on the black box model, the finite element method (FEM) has been applied to an IPMC actuator in order to predict the complete mechanical behavior of an actuator. Lee *et al*[17] and Metz *et al*[18] used the thermal analogy method to solve the problem successfully. Yoon e*t al*[19] solved the ion and water molecule transport equation using a thermal analogy to predict the bending behavior of an IPMC actuator.

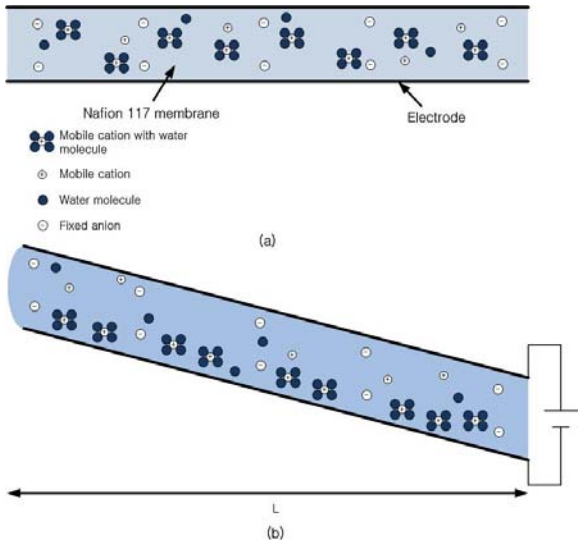

Fig. 1 Ion movement under the electric fields in Nafion 117: (a) cross section composition (b) ion migration

Predicting the bending behavior of an electro-active polymer has always been a difficult and complicated task. Systems involve multiple energy domains and various differential equations with different variables are difficult or impossible to solve analytically. Numerical methods are frequently used in an attempt to predict the swelling response, but these are also usually limited by the number of equations involved. Although various models, as described above, have been proposed from different physical points of view, none has yet been fully established.

In the present study, we assume that the bending of an IPMC beam, upon the applied electric field across its thickness, is dominated by ion and water content redistribution. When an electric potential is applied to the IPMC electrode, cations migrate to the cathode while anions remain stationary because they are covalently fixed to the membrane. Cations and water molecules are concentrated near the cathode and are deficient near the anode while moderate concentration is maintained in most of the membrane. Therefore, a very steep water concentration gradient develops near the electrodes, and this near electrode region is called the concentrated ion boundary layer. Two boundary layers that have similar thickness are characterized as the cation-deficient anode boundary layer and the cation-surplus cathode boundary layer. The two boundary layers effectively balance the applied electric field, resulting in the region between the two layers being shielded. Swelling due to migration of water molecules causes strain in the boundary layers, which causes bending deformation of an IPMC beam. Analytical consideration of ion and water molecule transport provides physical reasons for the physicochemical phenomena under the applied electric field. However, determining various parameters, including the chemical, physical, electrical, and mechanical properties of IPMCs requires formidable experimental work and assumptions. Since the concentration distribution profiles are symmetric and linear in the very thin region of the cathode and the anode,[20] the concentration boundary layer thickness can approximately determine the water molecule distributions and strains caused by swelling.

We have developed a new modeling method that can determine the thickness of the concentration boundary layer based on the experimentally measured tip displacement of an IPMC beam. This model determines the virtual boundary layer thickness, and the electrochemical phenomena behind the IPMC operations are not explored. We use a thermal analogy in which temperature is mimicked with voltage and ion distribution is mimicked with temperature distribution, which is similar to the method used by previous researchers.[17,18] The previous bimorph beam model requires two experimental parameters (tip displacement and blocking force) to determine the modeling parameters (the electromechanical coupling coefficient and the equivalent Young's modulus). Since our model requires only one experimental parameter (tip displacement) to determine the stress and strain distribution for an IPMC beam, our model can be applied to analyze the mechanical behavior of various types of IPMC actuators without measuring the blocking force at the tip.

In this study, the concentrated ion boundary layer model is presented as a black box model. The calculation results of our model are compared to those of a conventional equivalent bimorph beam model. The purpose of this study is to generalize the complex physical problem regarding ion transportation and strain generation, and minimize the experimental parameter for numerical modeling of an IPMC beam. Section 2 contains the theoretical basis for this model. Experimental procedures are summarized in section 3. The bimorph beam model is simulated in section 4. Procedures for the concentrated boundary layer model are presented in section 5, and the results of numerical studies are shown in section 6. Section 7 is the discussion and conclusion.

2. Basic Theories

2.1 Charge Redistribution

As mentioned before, the primary cause of IPMC bending under applied voltage is ion redistribution. The time variation of the

charge distribution is governed by the following equation.[21]

$$\frac{\partial}{\partial x}\left\{\frac{\partial k_{\varepsilon}E_2}{\partial t}-D^{+}\left[\frac{\partial^2\left(k_{\varepsilon}E_2\right)}{\partial z^2}-\frac{C^{-}F^2}{K_eRT}\left(k_{\varepsilon}E_2\right)\right]\right\}=0 \qquad (1)$$

where E_2 is the electric field, k_e is the electric permittivity, D^+ is the cation diffusivity coefficient, R is the general gas constant, T is the temperature, C^- is the anion charge density and F is the Faraday constant.

The density of water molecules $w(x, y, t)$ can be calculated by the following equation.[21]

$$\frac{\partial w(x,y,t)}{\partial t}=\frac{kT}{\eta}\left\{\frac{\partial^2 w(x,y,t)}{\partial x^2}+\frac{\partial^2 w(x,y,t)}{\partial y^2}\right\} \qquad (2)$$

Here k is the Boltzmann constant, T is the temperature and η is the viscosity coefficient for free water molecules. Once the water molecule density distribution is known, strain induced by swelling can be obtained. Tadokoro and Popovic[22,23] give the linear relationship between the strain (ε) and the relative water density (W) by experimental work as follows:

$$\varepsilon_i^x=\varepsilon_i^y=\varepsilon_i^z=C_wW \qquad (3)$$

Here, C_w is the experimental constant, and W is the relative water density. Relative water density is defined by the actual water content normalized by the standard water content that is calculated with the density of the hydrated Nafion membrane density and the element volume.

2.2 Thermal Analogy

Bending of an IPMC beam can be estimated by thermal analogy. A thermo-structural coupled field in ANSYS program (Taesung S&E Inc., Seoul, Korea) is used to simulate the electro-structural coupled field of an IPMC beam. When the temperature difference is applied across an IPMC strip, the thermally induced strain (ε_{th}) can be expressed as follows:

$$\varepsilon_{th}=\alpha\left(T-T_{ref}\right) \qquad (4)$$

where α is the thermal expansion coefficient, T is the temperature, and T_{ref} is the reference temperature. Strain induced by the prescribed electric field through the thickness direction is given by the following equations:

$$\varepsilon_V=d_{21}\frac{\Delta V}{t} \qquad (5)$$

where d_{21} is the electromechanical coupling coefficient, ΔV is the electric potential and t is the thickness of the IPMC membrane. When thermally induced strain is equivalently replaced by electrically activated strain, we can derive the following expression from equations (4) and (5):

$$\alpha\Delta T\leftrightarrow\frac{d_{21}}{t}\Delta V \qquad \alpha\approx\frac{d_{21}}{t} \qquad (6)$$

$$\Delta T=q\frac{L}{KA} \qquad V=iR=i\frac{\rho L}{A} \qquad (7)$$

where k is the thermal conductivity, q is the heat flux, A is the cross-sectional area, L is the length, i is the current and ρ is the electrical resistivity. From equations (7) with the analogy of ΔT and V, and q and i, we can derive the following:

$$k\approx\frac{1}{\rho} \qquad (8)$$

2.3 Finite Element Analysis

In classical structure analysis, the equations of the theory of elasticity are based on Hooke's law expressed as follows:

$$\{\varepsilon\}=\begin{Bmatrix}\varepsilon_x\\ \varepsilon_y\\ \varepsilon_z\\ \gamma_x\\ \gamma_y\\ \gamma_z\end{Bmatrix} \quad \{\sigma\}=\begin{Bmatrix}\sigma_x\\ \sigma_y\\ \sigma_z\\ \tau_x\\ \tau_y\\ \tau_z\end{Bmatrix} \quad \{\sigma\}=[K]\cdot\{\varepsilon\} \qquad (9)$$

where strain ε and stress σ in the body are linked by the deformation matrix [K]. Strain can also be related linearly by equation (9) to the applied voltage in the electro-mechanical system. To take into account the interaction between mechanical behavior and the electrical actuation principle, we can express the electro-elasticity equation as follows:

$$\begin{aligned}\{\sigma\}&=[K]\cdot\left(\{\varepsilon-\varepsilon_V\}\right)\\ \{\varepsilon_V\}&=\frac{d_{21}}{t}\cdot V\cdot\begin{bmatrix}1 & 1 & 1 & 0 & 0 & 0\end{bmatrix}^{T_r}\end{aligned} \qquad (10)$$

where T_r is the transpose of the vector. ANSYS does not provide a module for this particular equation, but includes the couple field analysis based on the theory of thermo-elasticity. This analysis takes into account the interaction between the mechanical and thermal fields and uses the following equations:

$$\begin{aligned}\{\sigma\}&=[K]\cdot\left(\{\varepsilon-\varepsilon_{th}\}\right)\\ \{\varepsilon_{th}\}&=\alpha\cdot T\cdot\begin{bmatrix}1 & 1 & 1 & 0 & 0 & 0\end{bmatrix}^{T_r}\end{aligned} \qquad (11)$$

where T (x, y, z) is the non-uniform temperature field in the body. In this study, we mimic the voltage by the temperature, and the thermal expansion coefficient by the electromechanical coupling coefficient (Eq. (6)). ANSYS combines each element's strain equation to find the form of the structure made up of these elements. This couple field analysis takes into account the influence of an external factor on a classical structure analysis. In this case, ion concentration in the upper and lower layers of an IPMC beam induces internal forces in the model. Solid5 couple field elements are used for the calculation that includes the coupling effect in ANSYS. Solid5 has a 3-D magnetic, thermal, electric, piezoelectric, and structural field capability with limited coupling between the fields. The element has eight nodes with up to six degrees of freedom at each node. The following matrix equation describes the coupling effect:

$$\begin{bmatrix}[K_{11}] & [K_{12}]\\ [K_{21}] & [K_{22}]\end{bmatrix}\begin{Bmatrix}\{X_1\}\\ \{X_2\}\end{Bmatrix}=\begin{Bmatrix}\{F_1\}\\ \{F_2\}\end{Bmatrix} \qquad (12)$$

where subscripts 1 and 2 represent one and other physics, respectively. The coupling effect can be seen in $[K_{12}]$ and $[K_{21}]$. ANSYS solves the model by the method based on iteration and using convergence analysis.[24]

3. Experimental Procedures

Nafion®-117 film with a thickness of 0.18 mm from Dupont (New Castle, DE, United States) was used as the ionic polymer membrane. Samples were manufactured by packing Nafion films under pressure and heat. Five and six films were used to manufacture samples A and B. For hot pressing, Nafion films were placed between the presses, heated up, and pressed with medium pressure. The detailed steps were described in the reference.[25] Manufactured Nafion samples were electroplated with platinum by using an impregnation-reduction reaction. The thickness of an electrode was on the order of a few micrometers; therefore it does not affect the sample thickness. The prepared sample was fixed in the edged vice, and cut with a razor blade into 1-mm widths. The experimental apparatus was composed of a laser displacement measurement system (CP08MHT80, Wenglor Sensors Ltd., United States), a potentiometer to induce voltage, a load cell (2002 NICOM IPMC controller, NICOM Ltd., Korea), and a personal computer system to control the instrumentation (shown in Fig. 2). The IPMC was cantilevered at one end as shown in Fig. 3. The free lengths (L) for strips A and B were 30 mm. The sample was fully hydrated in water, and the experiment was performed in air within two hours. The tip displacement was measured by the laser displacement measurement system, and the tip force (blocking force) of an IPMC specimen under applied voltage was measured by the load cell.

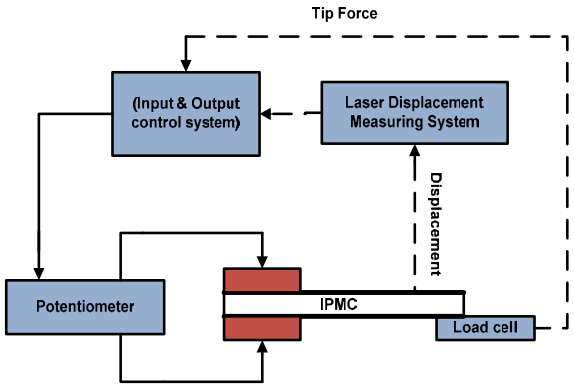

Fig. 2 Schematic diagram of displacement and force measurement system

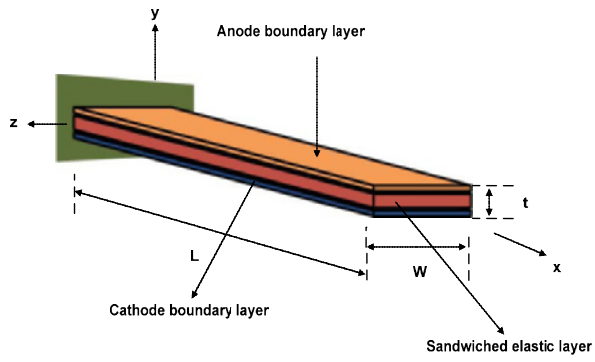

Fig. 3 IPMC strip with three virtual layers

4. Equivalent Bimorph Beam Model

Generally, for a cantilevered bimorph beam with a sandwiched elastic layer, the tip displacement (s) and the blocking force (F_B) can be written as follows:[15]

$$S = \frac{3L^2}{2t}\frac{(1+b)(2b+1)}{ab^3+3b^2+3b+1}d_{21}E_2 \tag{13}$$

$$F_B = \frac{3Wt^2E}{8L}\frac{2b+1}{(b+1)^2}d_{21}E_2 \tag{14}$$

where a and b are the Young's modulus ratio and the thickness ratio of the sandwiched elastic layers and outer layers, respectively. E_2 is the electric field and d_{21} is the electromechanical coupling coefficient in which subscripts 1 and 2 stand for the x-direction and the y-direction. If there is no elastic layer and input voltage V is replaced by tE_2, then the tip displacement and blocking force can be written as follows:[17]

$$S = \frac{3L^2}{2t^2}d_{21}V \tag{15}$$

$$F_B = \frac{3WtE}{8L}d_{21}V \tag{16}$$

As explained earlier, equations (15) and (16) give the tip displacement and blocking force for a bimorph beam, respectively. From these equations, we can deduce electromechanical coupling, which is given as follows:

$$d_{21} = \frac{2sH^2}{3L^2V} \tag{17}$$

Lee *et al*[17] calculated the equivalent of Young's modulus from equation (16), and used it to reproduce the force-displacement relationship of an actuator. The numerical results agreed well with the measured data. The equivalent bimorph beam model is very attractive and convenient, but it requires two experimentally measured data - tip displacement and blocking force. If we calculate the electromechanical coupling coefficient using tip displacement from equation (17) and use the material property of IPMC, the force-displacement relationship of an IPMC actuator can be effectively obtained.

We modeled bending behavior of an IPMC strip by using the thermal analogy in the ANSYS program. The electromechanical coupling and thermal expansion coefficient were determined by equations (17) and (6), respectively. Here, t was defined as the half of beam thickness in a bimorph model. The volume fraction of platinum layer (1 micron each side) was about 0.0018 for the 1.1 mm thick IPMC strip, and Young's modulus was estimated at about

300 MPa by the rule of mixture. However, the platinum layer was less uniform along its thickness, and the rigidity of platinum layer contributed less to the composite. In this study, Young's modulus and Poisson's ratio were set to be 230 MPa and 0.49 for IPMC strips, which was close to the material properties of Nafion film, and these values were also used in ref.[20,26]

Table 1 shows the results of this simulation. The errors were less than 8% for the simulated and experimental tip displacements. The error in the blocking force was more significant. The possible reason for the error was due to the modulus of elasticity, which could be computed by equation (16) in the case of the conventional bimorph model. Equation (16) showed the modulus of elasticity depended on experimental results, and it might be different for different IPMC strips. Using the material property of Young's modulus would not be appropriate in the equivalent bimorph model, but we used the physical material property in order to simulate the case where the experimental data for the blocking force was not available.

5. Concentrated Ion Boundary Layer Model

When an electric potential is applied to the IPMC electrode, cations and water molecules migrate to the cathode and are concentrated near the cathode and deficient near the anode. Stresses will develop in the upper and lower boundary layers, leading to deformation of an IPMC beam. With reference of the redistribution of cations and associated water under the applied electric field in this model, it can be assumed that an IPMC beam has three virtual layers (shown in Fig. 3). The anode and cathode concentration boundary layers, where water concentration has a large gradient, primarily contribute to the bending motion of an IPMC. A very steep water concentration gradient develops inside the region near the electrode, which is called the concentrated ion boundary layer whereas a negligible gradient is maintained in the middle layer. The thickness of the concentration boundary layer can be obtained by solving the water transport equation, but complex equations should be solved simultaneously, and various physicochemical parameters must be determined. The concentration distribution is symmetric over the neutral axis and has a negligible gradient in most of the membrane except the thin boundary layer; therefore, linear concentration distribution inside the boundary layer is a good approximation.[14,20] The thickness of the concentrated ion boundary layer is determined by the iteration method using the experimentally measured tip displacement instead of solving complex transport equations.

To solve the strain induced by water molecule redistribution in ANSYS, we draw an analogy between the thermal strain and real strain in IPMC due to the volume change. The coupled structure/thermal model of ANSYS is used to solve the stress and strain distribution in the IPMC samples. The flowchart in Fig. 4 shows the steps involved in establishing a model based on ANSYS analysis.

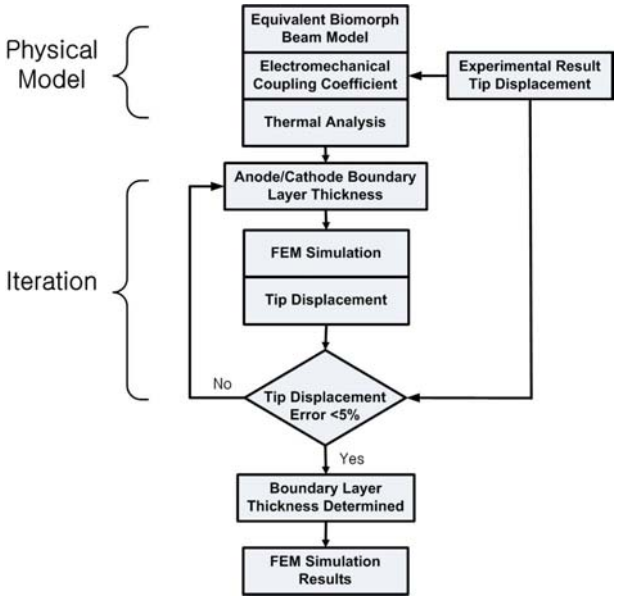

Fig. 4 Flowchart for model establishment

For a given sample, the electromechanical coupling coefficient is calculated using the experimentally measured tip displacement. The concentrated ion boundary layer thickness is assumed. Using the thermal analogy of the electromechanical system, thermal loading is applied as a boundary condition. Stress and strain fields are analyzed, and the calculated tip displacement is compared to the experimental one. If the two values are different, the boundary layer thickness is adjusted, and the strain field is simulated until the calculated and measured tip displacement agree well (within 5% error). Boundary layer thickness is usually in the range of 20 to 100 micrometers, and it is usually determined within ten iterations. Once the boundary layer thickness is determined, the stress and strain distribution in the IPMC strip is finally analyzed. The prime goal of this study is to generalize the complex physical problems regarding ion transport and strain development under the applied electric fields and minimize the number of experimental parameters for IPMC beam bending modeling. We tried to achieve this target by adjusting the anode/cathode boundary layer thickness based on the experimentally measured tip displacement.

Table 1 Comparison of tip displacement and blocking force for the equivalent bimorph beam model and the experiment

IPMC thickness (μm)	IPMC free length/width(mm)	Thermal expansion coefficient($1/^{o}C$)	Voltage (V)	Tip displacement Experiment (mm)	Tip displacement Simulation (mm)	Blocking force Simulation (g_f)	Blocking force Experiment (g_f)
A(920)	30/1	0.0022	3	4.90	5.29	0.28	0.36
		0.0031	4	9.10	9.85	1.04	1.11
B(1120)	30/1	0.0017	3	5.57	6.00	0.68	0.48
		0.0023	4	9.71	10.4	1.21	1.22

5.1 Thermal Conductivity

As the voltage input of an IPMC beam is analogous to the temperature in the thermal analogy model, it is needed to create the temperature difference across the IPMC in thickness direction. As equation (8) shows the analogy between thermal conductivity and electrical permittivity, the thermal conductivity for anode/cathode boundary layers is selected as 1 x 10^9 W/m^{o}C, which is the inverse of the electrical resistivity of IPMC. With reference to operational principle of IPMC, the concentration gradients of water and cation develop in the boundary layers near the electrodes. Since the temperature (or voltage) gradient is analogous to the ion concentration gradient, there is a negligible ion concentration gradient outside the boundary layer. We can achieve a flat gradient by increasing the thermal conductivity outside the boundary layer. If we increase the thermal conductivity up to 1 x 10^{13} W/m^{o}C, a negligible temperature gradient is formed. Further increase in the thermal conductivity does not change the temperature gradient. The temperature profile for the selected thermal conductivity value in strip B (under 4 volt) is shown in Fig. 5.

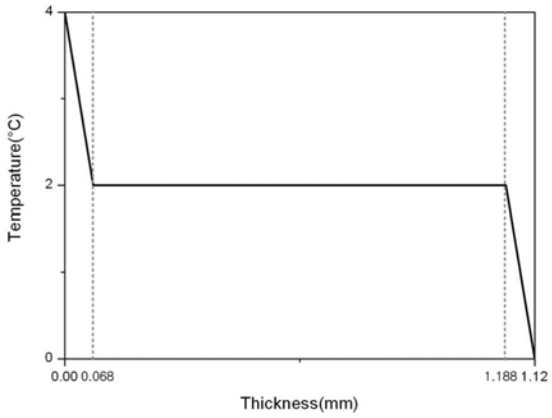

Fig. 5 Temperature distribution along the thickness of the IPMC (Model B, 4V)

5.2 Thermal Expansion Coefficient

It is believed that an electromechanical reaction is more effective near the vicinity of electrodes. This is mainly due to high water concentration in the anode/cathode boundary layers. The water molecules migrate to the electrodes and diffuse back to the membrane. Based on the strain generated by water molecule movement and the analogy of concentration and temperature, equations (3) and (4) are compared as follows:

$$\alpha \approx \frac{C_w W}{\Delta T} = \frac{C_w W}{(T - T_{ref})} \tag{18}$$

Here, C_w is the experimental constant and W is the relative water density. $W = m_{ij}/m_r = 10^{-5}\, x$, where x is the water density distribution per 1 V. m_{ij} is the actual water content, and $m_r = v\, \rho_w$ is the standard water content calculated with the density of the hydrated Nafion membrane (ρ_w) and element volume v. The value x in the concentration boundary layer and C_w is taken from[20] as x =2000 mole/m^3/μm and C_w = 0.8. In equation (4), the thermally induced strain is proportional to ΔT which is the temperature difference between the real and reference temperatures. T_{ref} is selected as the mean value of the temperatures at both boundaries. Expansion near the anode and contraction near the cathode are simulated inside the boundary layers while negligible strain develops in most of the middle layer.

5.3 Model Parameters

The concentrated ion boundary layer thickness was adjusted to develop close correspondence between experimental and theoretical tip displacement. The anode/cathode boundary layer thickness was adjusted so that simulated tip displacements were close to the experimental results within 5% error. Three virtual layers - the anode boundary layer, the middle layer and the cathode boundary layer -were assumed in a strip with reference to ion concentration. Thermal conductivity of each layer was imposed. The mechanical properties, Young's modulus and Poisson's ratio, were set to be 230 MPa and 0.49 for Nafion. Meshing of the model was done with solid 5 couple field element type, and the effect of large deformation was accounted for. Temperature boundary conditions were applied to the upper and lower surfaces of an IPMC strip. The simulation ran properly with nearly 1000 elements and took about 2 min to converge. We used non-uniform meshes in the y direction - fine meshes near the cathode and anode and coarse meshes near the neutral layer. Further refinement of the meshes did not affect the analysis results. Finite element analysis with the concentrated ion boundary layer was performed. To calculate the blocking force (reaction force) at the tip of the IPMC, the contact element was used. With contact 175 and target 170 elements, static non-linear analysis for node-to-surface contact was performed.

6. Results

6.1 Boundary Layers Thickness

Once we standardized all the parameters using the voltage to temperature analogy and the temperature to ion concentration analogy, the next step was determining the anode/cathode boundary layers thickness. We could adjust the tip displacement by iteratively changing the anode/cathode boundary layer thickness in the ANSYS simulation until the simulated tip displacement coincided with the measured one. Table 2 shows the anode/cathode layer thickness for strips A and B under different applied voltages. It suggested that the anode/cathode boundary layer thickness increased as applied voltage and thickness of IPMC sample increased. Relative boundary layer thickness, which was the boundary layer thickness divided by the sample thickness, also

Table 2 Boundary layer (BL) thickness for strips A and B

Strips	Voltage (V)	BL thickness (μm)	Relative BL thickness (%)	Increase of BL per 1V (%)
A	3	30	6.5	38.6
	4	42	9.1	
B	3	51	9.1	33.3
	4	68	12.1	

increased as the sample thickness increased. The increase in the anode/cathode boundary layer per 1V was about 39% and 33% for strips A and B, respectively. The percentage increase of the boundary layer thickness per volt had similar values for the tested samples.

6.2 Blocking Force

To calculate the actuation force (reaction force) at the tip of the IPMC, the contact element was used. The displacement contour is shown in Fig. 6 for Model B, and the reaction forces are shown in Fig. 7. Table 3 shows the calculated blocking forces and experimentally measured blocking forces for different strips. The results suggest that the blocking force increases as the voltage and sample thickness increases. This finding agrees with the previous workers' experimental results.[17,25,27] The simulated blocking forces also agree well with our experimental results. The maximum error is less than 13%, which is within the reasonable range considering the experimental errors.

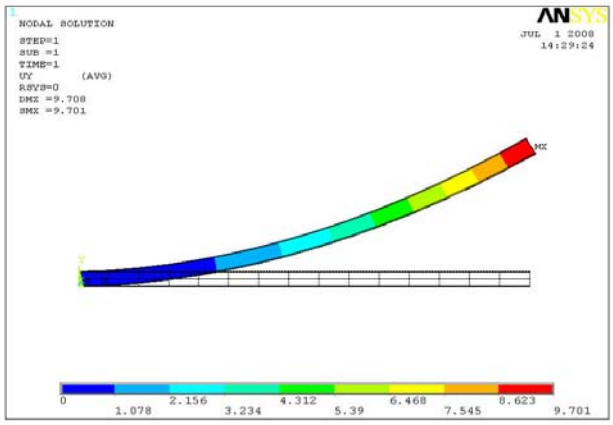

Fig. 6 Contour plot of displacement for model B (4 volt)

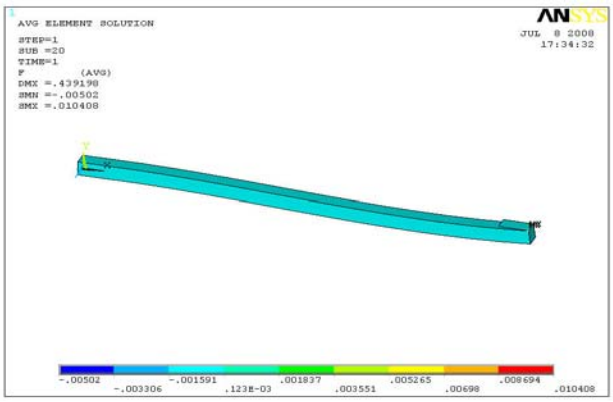

Fig. 7 Contour plot of force for model B (4 volt)

7. Discussion and Conclusion

We modeled and analyzed the bending behavior of an IPMC beam by establishing a new computational model based on the concentration boundary layer thickness of water molecules for finite element analysis. The model divided an IPMC beam into three virtual layers. We assumed that bending deformation in an IPMC beam occurred due to stress generation in the anode and cathode boundary layers, which was caused by ion and water migration to the electrodes. Since the movement of cations and water molecules is associated with the stress and strain generated in IPMCs, the degree of hydration is very important in the applications of IPMC as an actuator. Encapsulation of IPMC to prevent dehydration of IPMCs is a critical issue nowadays. Various efforts have been performed using SaranR plastic membrane,[28] PDMS,[29] dielectric gel,[30] but the hydration of IPMCs still limits the application of IPMCs.

To analyze the deformation characteristics of an IPMC beam using ANSYS, we used thermal analogy in which the temperature was mimicked with the voltage and the ion concentration distribution was mimicked with the temperature distribution. Once all parameters were standardized with reference to physical material properties, tip displacement depended only upon the anode/cathode boundary layers thickness. The boundary layer thickness was adjusted until the calculated tip displacement agreed with the experimental one. The determined anode/cathode boundary layer thickness and physical properties were used in the finite element model to get the blocking force, and the numerical results from finite element analysis were compared with the experimental ones. The results showed that the boundary layer thickness increased as the applied voltage increased for the same sample. The boundary layer thickness also increased as the sample thickness increased, but the percentage increase of the boundary layer thickness per volt has similar values for the tested samples. Since we have experimental data in the limited voltage range, further study will be required. Both tip displacement and blocking force increased with increase of anode/cathode boundary layer thickness and applied voltage. The simulated blocking force agreed well with the experimental data. The maximum error was less than 13%, which is within the reasonable range considering the experimental errors. Standard deviations of experimental data were about 10% because of the inconsistent mechanical behavior of the IPMC samples due to individual variations in water content and fatigue cause by repeated experiments.

The simulated blocking forces using an equivalent bimorph beam model deviated more from the measured data as shown in

Table 3 Comparison of tip displacement and blocking force for the concentrated ion boundary layer model and he experiment

IPMC thickness (μm)	IPMC free Length/width (mm)	Boundary layer thickness (μm)	Voltage (V)	Tip displacement Experiment (mm)	Tip displacement Simulation (mm)	Blocking force Simulation (g_f)	Blocking Force Experiment (g_f)
A(920)	30/1	30	3	4.90	4.90	0.39	0.36
		42	4	9.10	9.06	0.95	1.11
B(1120)	30/1	51	3	5.56	5.57	0.46	0.48
		68	4	9.70	9.71	1.06	1.22

Table 1. If we used the Young's modulus calculated from the measured blocking force as in the conventional bimorph model, the simulated blocking force might show good agreement with the experimental data. In this study, we assumed the case in which measured blocking forces were not available.

The proposed ion boundary layer model promises a possibility of modeling and analyzing IPMC behavior with one modeling parameter to be determined. Experimental data such as tip displacement and blocking force are required to determine the model parameters, such as electro-mechanical coupling coefficient and Young's modulus in the equivalent bimorph beam model. In the concentrated ion boundary layer model, two parameters (the electro-mechanical coupling coefficient and the boundary layer thickness) are to be determined, but the boundary layer thickness can be estimated by comparing the simulated tip displacement to the experimental data. The proposed model is effectively applicable to the case where only experimentally measured tip displacement is available without blocking force measurement.

In conclusion, we draw an analogy between thermal strain and real strain in IPMCs due to volume change. The effect of the concentration of ions in the IPMC boundary layer is mimicked with the temperature, and the electromechanical coupling coefficient is mimicked with the thermal expansion coefficient. A concentrated ion boundary layer model is developed, which requires only one experimental data (tip displacement) to determine the model parameters. The theoretical and experimental results demonstrate that the suggested model is practical and effective enough in predicting the tip displacement and blocking force of IPMC strips for different input voltages and strip thicknesses.

ACKNOWLEDGEMENT

This study was supported by a grant from the Seoul Development Institute (New Technology Research and Development Program 2006-10979).

REFERENCES

1. Cohen, Y. B., "Electric flex," IEEE Spectrum, Vol. 41, No. 6, pp. 29-33, 2004.
2. Tadokoro, S., Yamagami, S. and Ozawa, M., "Soft micromanipulation device with multiple degrees of freedom consisting of high polymer gel actuators," Proc. of IEEE International Conference on Micro Electro Mechanical Systems, pp. 37-42, 1999.
3. Guo, S., Fukuda, T. and Asaka, K., "A new type of fish-like underwater microrobot," IEEE/ASME Transactions on Mechatronics, Vol. 8, No. 1, pp. 136-141, 2003.
5. Shahinpoor, M. and Kim, K., "Ionic polymer-metal composites: IV. Industrial and medical applications," Smart Materials and Structures, Vol. 14, No. 1, pp. 197-214, 2005.
6. Yamakita, M., Kamamichi, N., Kozuki, T., Asaka, K. and Luo, Z., "Control of biped walking robot with IPMC linear actuator," Proc. of the IEEE/ASME International Conference on Advanced Intelligent Mechatronics, pp. 48-53, 2005.
7. Tan, X., Kim, D., Usher, N., Laboy, D., Jackson, J., Kapetanovic, A., Rapai, J., Sabadus, B. and Zhou, X., "An autonomous robotic fish for mobile sensing," Proc. of the IEEE/RSJ International Conference on Intelligent Robots and Systems, pp. 5424-5429, 2006.
8. Chen, Z., Shen, Y., Xi, N. and Tan, X., "Integrated sensing for ionic polymer-metal composite actuators using PVDF thin films," Smart Materials and Structures, Vol. 16, No. 2, pp. S262-S271, 2007.
9. Rolfe, P., Sun, J., Scopesi, F. and Serra, G., "Bioengineering aspects of sensors and Instruments for continuous monitoring of the venitilated newborn," IJPEM, Vol. 10, No. 1, pp. 49-54, 2009.
10. Zhou, J. W. L., Chan, H.-Y., To, T. K. H., Lai, K. W. C. and Li, W. J., "Polymer MEMS actuators for underwater micro-manipulation," IEEE/ASME Transactions on Mechatronics, Vol. 9, No. 2, pp. 334-342, 2004.
11. Shahinpoor, M., "Micro-electro-mechanics of ionic polymer gels as electrically controllable artificial muscles," J. Intell. Mater. Syst. Struct., Vol. 6, No. 3, pp. 307-314, 1995.
12. Nemat-Nasser, S. and Li, J. Y., "Electromechanical response of ionic polymer-metal composites," J. Appl. Phys. Vol. 87, No. 7, pp. 3321-3331, 2000.
13. Nemat-Nasser, S., "Micromechanics of actuation of ionic polymer–metal composites," J. Appl. Phys., Vol. 92, No. 5, pp. 2899-2915, 2002.
14. Johnson, T. and Amirouche, F., "Multiphysics modeling of an IPMC microfluid control device," Microsys. Technol., Vol. 14, No. 6, pp. 871-879, 2008.
15. Wang, Q. and Xu, B., "Nonlinear piezoelectric behavior of ceramic bending mode actuator under strong electric fields," J. Appl. Phys., Vol. 86, No. 6, pp. 3352-3360, 1999.
16. Xiao, Y. and Bhattacharya, K., "Modeling electromechanical properties of ionic polymers," Proc. SPIE, Vol. 4329, pp. 292-300, 2001.
17. Lee, S., Park, H. C. and Kim, K. J., "Equivalent modeling for ionic polymer-metal composite actuators based on beam theory," Smart Materials and Structures, Vol. 14, No. 6, pp. 1363-1368, 2005.
18. Mets, P., Alici, G. and Spinks, G. M., "A finite element model for bending behavior of conduction polymer electromechanical actuators," Sensors and Actuators A: Physical, Vol. 130-131, pp.

1-11, 2006.

19. Yoon, W. J., Reinhall, P. G. and Seibel, E. J., "Analysis of electro-active polymer bending: A component in a low cost ultrathin scanning endoscope," Sensors and Actuators A: Physical, Vol. 133, No. 2, pp. 506-517, 2007.
20. Toi, Y. and Kang, S-S., "Finite element analysis of two-dimensional electrochemical-mechanical response of ionic conduction polymer-metal composite beams," Computers and Structures, Vol. 83, No. 31-32, pp. 2573-2583, 2005.
21. Nemat-Nasser, S. and Li, J. Y., "Electromechanical response of ionic polymer composites," Proc. of SPIE, Vol. 3987, pp. 82-91, 2000.
22. Tadokoro, S., Takamori, T. and Oguro, K., "An actuator model of ICPF (Ionic Conducting Polymer Film) for robotic applications on the basis of physicochemical hypotheses," Proc. of 2000 IEEE international conference of robotics and automation, Vol. 2, pp. 1340-1346, 2000.
23. Popovic, S. and Taya, M., "Modeling of Nafion-Pt actuator in dry condition," Ph.D. thesis, Department of Mechanical Engineering, University of Washington.
24. ANSYS, "Various couple field analysis using ANSYS: Training Manual," 2005.
25. Lee, S. J., Han, M. J. and Kim, Y. H., "A new fabrication method for IPMC actuators and application to artificial fingers," Smart Materials and Structures, Vol. 15, No. 5, pp. 1217-1224, 2006.
26. Kim, J. K. and Shahinpoor, M., "Ionic polymer-metal composite: II. Manufacturing Techniques," Smart Materials and Structures, Vol. 12, No. 1, pp. 65-79, 2003.
27. Lee, S. G., Park, H.-C., Pandita, S. D. and Yoo, Y., "Performance improvement of IPMC (Ionic Polymer Metal Composites) for a flapping actuator," International Journal of Control, Automation, and Systems, Vol. 4, No. 6, pp. 748-755, 2006.
28. Akle, B. and Leo, D. J., "Electromechanical transduction in multilayer ionic transducers," Smart Materials and Structures, Vol. 13, No. 5, pp. 1081-1089, 2004.
29. Malone, E. and Lipson, H., "Freeform fabrication of electroactive actuators and electromechanical devices," Proc. of the 15th Solid Freeform Fabrication Symposium, pp. 697-708, 2004.
30. Barramba, J., Silva, J. and Costa Branco, P. J., "Evaluation of dielectric gel coating for encapsulation of ionic polymer-metal composite (IPMC) actuators," Sensors and Actuators A: Physical, Vol. 140, No. 2, pp. 232-238, 2007.